Journal of Applied Mechanics and Technical Physics, Vol 35, No 3, 1994

ANISOTROPY FROM SLIPPINGS

V. M. Zhigalkin and B. A. Rychkov

UDC 539.37

The need to complete the theory of slipping with reliable experimental results [2] has recently been acknowledged [1].

In this paper, as in [3], we develop a model of a material in which plastic deformation is represented as the result of slippings over the area of the principal shear stresses. Specially set up experiments on thin-walled tubular specimens of 40Kh steel provided the means for completely verifying and supplementing the parameters introduced into this model and of checking its predictions regarding the nature of the strain anisotropy that occurs in the material.

1. We will consider the stress-strain state of an element of a solid for fixed directions of the principal axes of the stress tensor. This state occurs in experiments on the stretching (or compression) of thin-walled tubes with internal pressure. We will denote the axial stress in this specimen by σ_z, the circumferential stress by σ_φ, and the radial stress by $\sigma_r(\sigma_r \approx 0)$. Any of these principal normal stresses can become a maximum depending on the specified load trajectory; then, as is usually done, we will assign the subscripts 1, 2, 3 to them, where the following inequalities must be satisfied: $\sigma_1 > \sigma_2 > \sigma_3$. To this there correspond the principal shear stresses: the maximum $\tau_m = \tau_{13} = (\sigma_1 - \sigma_3)/2$ and $\tau_{12} = (\sigma_1 - \sigma_2)/2$, $\tau_{23} = (\sigma_2 - \sigma_3)/2$.

We used two-, three-, and four-section load trajectories in the space of the principal stresses in the experiment. The first section is a proportional load outside the elastic limit for a specified form of stress state. The latter will be characterized either by the Lode–Naday parameter for the stresses μ_σ, or by the invariant m, which is the ratio of the octahedral shear stress τ_0 to the maximum stress τ_m ($m = \tau_0/\tau_m$).

The following relation holds:

$$m = \sqrt{6 + 2\mu_\sigma^2}/3 \quad (\sqrt{2/3} \leq m \leq 2\sqrt{2/3}).$$

In addition, the invariant m can be represented in term of the angle of the form of the stress state χ_σ

$$m = \sqrt{\frac{2}{3}}/\sin\left(\chi_\sigma + \frac{1}{3}\pi\right) \quad (0 \leq \chi_\sigma \leq \pi/3).$$

Here the angle χ_σ is expressed in the well-known way in terms of the second and third invariants of the stress deviator.

We will use the following scheme of the slipping mechanism. For proportional loading, slippings occur in those areas of the principal shear stresses in which these stresses reach the values of the shear resistance S_{ij} [4]. The state that occurs will be a state of incomplete or complete plasticity [5, 6] depending on whether the condition $\tau_{ij} = S_{ij}$ is satisfied only over the area of maximum shear stress or over other extremal areas. These areas will henceforth be called slipping areas and will be denoted, like the shear stresses attached to them, by T_{ij}. For proportional loading $T_{ij} \equiv \tau_{ij}$. This identity in notation may break down under complex loading, since, for convenience in analyzing a succession of slippings, the notation of the slipping areas T_{ij} is preserved as it is taken on the first part of the loading trajectory. Thus, for loading in a state of pure shear ($\mu_1\sigma = 0$, $m = m_1\sqrt{2/3}$). Slipping initially occurs on the area T_{13}, denoted by T, i.e. $T \equiv \tau_m$. For further complex loading the maximum shear stress τ_m may "transfer" to the area T_{12} or T_{23}, and we can then speak of additional loading on these areas and of possible unloading over the area T etc.

2. Slippings which occur over areas of maximum shear stress are the main ones [4]. As was established in [3], the resistance to shear from these slippings for the loading considered has the form

$$S(\beta) = \psi(\tau_0, m) + \Psi(\tau_0, m)r(\beta) + A(1 - \cos 2\beta), \; A = \text{const}, \tag{2.1}$$

Novosibirsk. Translated from Prikladnaya Mekhanika i Tekhnicheskaya Fiziki, No. 3, pp. 136-144, May-June, 1994. Original article submitted June 8, 1993.

0021-8944/94/3503-0447$12.50

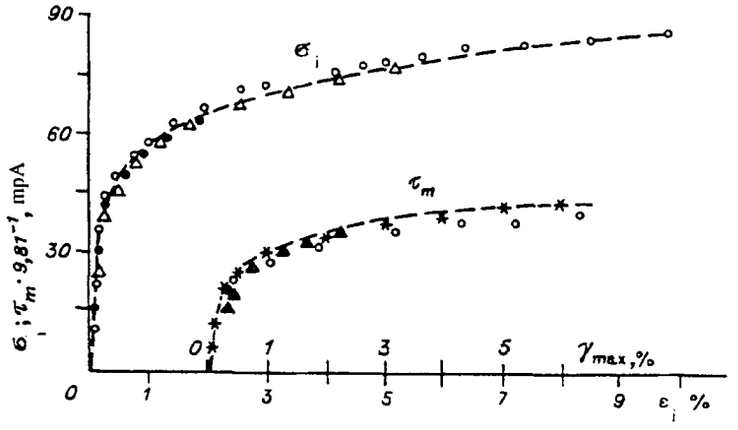

Fig. 1

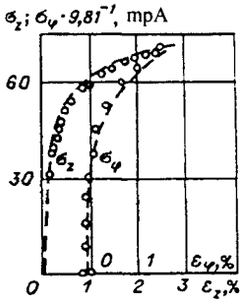

Fig. 2

where β is the direction of the slipping, measured from the direction of τ_m, $r(\beta)$ is the intensity of the main slippings, and ψ and Ψ are known functions of these arguments.

We will assume that the increments of the main strains from the main slippings $d\Gamma_i^0$ and the corresponding increments of all other possible slippings $d\Gamma_i^d$ are related as follows:

$$d\Gamma_1^d = (\tau_{12}/\tau_m)^q d\Gamma_1^0, \quad d\Gamma_3^d = (\tau_{23}/\tau_m)^q d\Gamma_3^0, \quad q = \text{const}, \tag{2.2}$$

where

$$d\Gamma_1^0 = -d\Gamma_3^0. \tag{2.3}$$

Summing the components (2.2) and (2.3) and taking into account the condition of incompressibility for purely plastic deformation, we obtain the total increments of its components along the principal axes

$$d\Gamma_1 = \left[1 + \left(\frac{\tau_{12}}{\tau_m}\right)^q\right] d\Gamma_1^0, \quad d\Gamma_3 = -\left[1 + \left(\frac{\tau_{23}}{\tau_m}\right)^q\right] d\Gamma_1^0,$$
$$d\Gamma_2 = \left[\left(\frac{\tau_{23}}{\tau_m}\right)^q - \left(\frac{\tau_{12}}{\tau_m}\right)^q\right] d\Gamma_1^0. \tag{2.4}$$

Summation of the elementary shears over all regions of the main slippings gives

$$d\Gamma_1^0 = \frac{1}{2}\int_{-\theta}^{\theta} dr(\beta)\cos 2\beta d\beta. \tag{2.5}$$

The limits of the fan of slippings $\pm\theta$ at the current instant of time t are found from the condition of continuity of their development, which is expressed either by equating the intensity of the slippings to zero within these limits in the case when

TABLE 1

Number of the readout point	σ_z	σ_φ	Γ_z	$-\Gamma_\varphi$	σ_n	τ_{12}	τ_{23}
	$9{,}81^{-1}$ MPa		%		$9{,}81^{-1}$ MPa		
9	42	0	0,191	0,100	42,0	21,00	0
10	43	2,5	0,196	0,099	41,8	20,25	1,25
11	44	5,0	0,205	0,103	41,7	19,50	2,50
12	45	7,5	0,215	0,105	41,7	18,75	3,75
13	46	10,0	0,223	0,106	41,9	18,00	5,00
14	47	12,5	0,239	0,105	42,1	17,25	6,25
15	48	15,0	0,258	0,104	42,5	16,50	7,50
16	49	17,5	0,280	0,098	43,0	15,75	8,75
17	50	20,0	0,303	0,097	43,5	15,00	10,00
18	51	22,5	0,338	0,096	44,2	14,25	11,25
19	52	25,0	0,381	0,093	45,0	13,50	12,50
20	53	27,5	0,432	0,088	45,9	12,75	13,75

there is a monotonic increase in the fan of slippings, or by the fact that the rate of change of this intensity in the case of partial "freezing" of the fan of slippings vanishes (in the directions $\pm\theta$). The intensity of the slippings is found from the condition for the resistance to shear (2.1) to be equal to the corresponding component of the shear stress $\tau(\beta)$ ($\tau(\beta) = \tau_m \cos 2\beta$) in the region where the slippings occur; outside this region $S(\beta) > \tau(\beta)$.

Hence, by specifying the trajectory of the loadings we can calculate the increments of the components of the plastic-deformation tensor from (2.4) and (2.5). As a result, we obtain relations similar to those in flow theory, which can only be integrated in the case of proportional loading. The elastic constituents of the deformation components are found from Hooke's law.

3. We took the following in the calculations:

$$\Psi(\tau_0, m) = p\left[\frac{(1 + 3m)\tau_m}{(1 + 3m_1)\tau_l} - 1\right]^c, \quad p, c = \text{const}; \tag{3.1}$$

$$\psi(\tau_0, m) = \frac{(1 + 3m_1)\tau_l - a\tau_0}{1 + (k - a)m}, \quad a = k - a_1/m, \; k, a_1 = \text{const} \tag{3.2}$$

(τ_l and m_1 are the yield point* and the value of the invariant m for pure shear, respectively).

The constant A in (2.1) for all the materials considered can be expressed [4] in the same way: $A = 4\tau_l$. A further four constants of the material occur in (3.1) and (3.2), namely, p, c, k, and a_1. The first pair (p and c) is found when approximating the hardening diagram by theoretical relations for pure shear (or for uniaxial stretching), since the function $\psi(\tau_0, m)$ plays the role of the secant modulus, and these diagrams are taken to be the listed characteristics of the material. Some information on the parameters k and a_1 are given below. Finally, the constant q in (2.4), like A, is taken to be the same for all materials: for $q = 0.75$ there is a difference between the Lode–Naday parameters for stresses and deformation observed in experiments for proportional loading.

The yield condition for an initially isotropic material follows from the condition for the resistance to shear to be equal to the maximum shear stress when $r(\beta) = \pm 0$, i.e. from the equation

$$\psi(\tau_0, m) = \tau_m.$$

It follows from the last expression, taking (3.2) into account, that there is a linear relationship between the maximum shear stress and the octahedral shear stress (which does not depend on the parameter a_1)

$$\tau_m = (1 + 3m_1)\tau_l - k\tau_0. \tag{3.3}$$

when $k = 0$ we obtain the Trask–Saint-Venant yield criterion and as $k \to \infty$ we obtain the Guber–Mises criterion. We took a value of k intermediate between the ones indicated ($k = 3$) in the calculations since it corresponds better to experimental data.

*We mean here by the field point, as usual in theoretical constructions, the point where the elastoplastic part of the hardening diagram joins the linear elastic part, defined, for example, by the Lode extrapolation method [7].

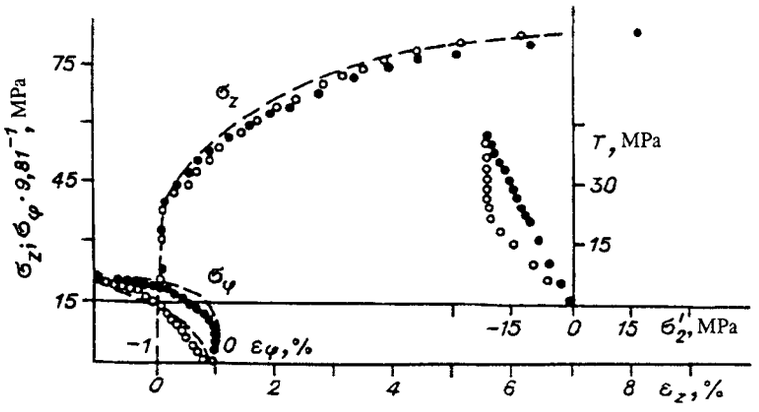

Fig. 3

Relation (3.3) reflects the following. At the instant when plastic deformation occurs the value of the maximum shear stress for pure shear is greater than its similar value for uniaxial stretching, while the octahedral shear stress, on the other hand, is less in the first case than in the second. If we assume this relationship to be preserved in the case of plastic deformation (for proportional loading) this means that the function (τ_0, m) in (2.1) must be a decreasing function as the stress level increases, which will characterize the quantity τ_0. The dependence of the deformation on the stress is as follows: for the same value of τ_m the shear Γ_{max} must be greater for uniaxial stretching than for pure shear. It is precisely this form of strengthening that is observed in the material considered. This is ensured in the model if the constant a_1 (see Eq. (3.2)) is positive. Its value can be found by taking into account the following property of the slipping scheme assumed.

Additional increments (2.2) of the components of plastic deformation arise from slippings over the areas T_{12} and T_{23}. It was established experimentally in [8] that the relations $\Gamma_{ij} = \Gamma_{ij}(T_{ij})$ ($i \neq j$, i, j = 1, 2, 3) are invariant. This means that the resistance to shear on any of the slipping areas T_{ij} can be represented by (2.1), which operates on the slipping intensity r_{ij} over the given area. As a result we can formulate the condition for slipping to occur and develop over any of the areas T_{ij} when there are basic slippings over the other areas. Using this approach the relation between the increments of the deformation from the main and additional slippings of the form (2.2) must be regarded as an approximation of the additional increments $d\Gamma_i^d$, which, in principle, can be calculated from the known resistance to shear. However, it is more convenient to use relation (2.2) since one then ensures, as already noted, the necessary relation between the Lode–Naday parameters for the stresses and strains.

For uniaxial stretching the main slippings are over the areas T and T_{12} (they are equally justified in this case). As the stress level increases or when there is a change in the form of the stress state, slippings may also occur over the area T_{23}. At this instant we have

$$\psi(\tau_0, m) = \tau_{23}^0, \tag{3.4}$$

where the stress $\tau_{23}{}^0$ must be regarded as the yield point on the given slipping area for a given level and form of the stressed state. Relation (3.4) also enables one to determine the constant a_1.

Thus, to determine a_1 the following loading program must be carried out: after uniaxial stretching, when $\tau_m = \tau_{12} > \tau_l$ and $\tau_{23} = 0$ (but the level of stresses is such that $\psi(\tau_0, m) > 0$), one must achieve changes of the form of the stressed state for which $\dot{\tau}_m = \partial\tau_m/\partial t > 0$, $\dot{\tau}_{12} < 0$, $\dot{\tau}_{23} > 0$. Slippings over the area T_{12} then cease, but will continue over the area T, and they will occur over the area T_{23} when condition (3.4) is satisfied. One can determine this instant experimentally by detecting the presence of an increment in the component Γ_2, since up to this instant a fixed value of the component Γ_2 (acquired in preliminary stretching) will correspond to pure shear strain due to slipping only over the area T.

4. In addition to this loading trajectory in an experiment to determine the initial properties of the material and the parameters of the model, one must also carry out five forms of proportional loading: 1) uniaxial stretching ($\sigma_z > 0$, $\sigma_\varphi = 0$, $\mu_\sigma = -1$); 2) stretching in a circumferential direction ($\sigma_\varphi > 0$, $\sigma_z = 0$, $\mu_\sigma = -1$); 3) compression when $\sigma_z = \sigma_\varphi$, $\mu_\sigma = 1$; 4) pure shear, when $\sigma_z = 2\sigma_\varphi$ or $\sigma_\varphi = 2\sigma_z$, $\mu_\sigma = 0$; 5) pure shear when $\sigma_z = -\sigma_\varphi$, $\mu_\sigma = 0$.

An experiment was carried out on thin-walled tubular specimens made of 40Kh steel.

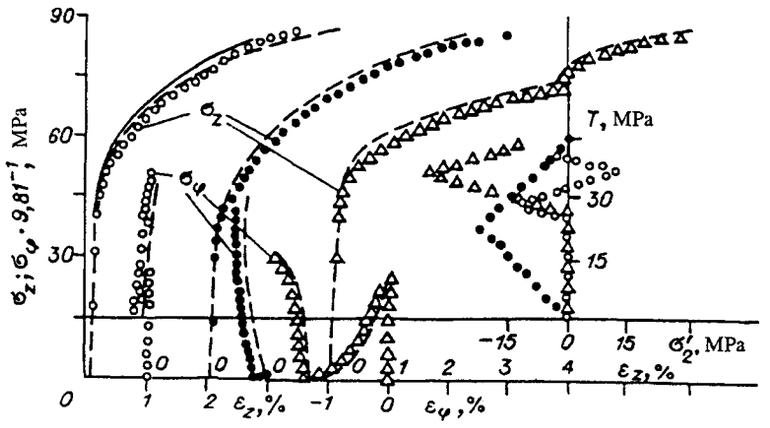

Fig. 4

Figure 1 shows a strengthening diagram of the material under test for proportional loading and calculated graphs obtained using the model for the following values of the material parameters: Young's modulus E = 21,500 × 9.81^{-1} MPa, Poisson's ratio $\nu = 0.32$, $\tau_l = 20 \times 9.81^{-1}$ MPa, $a_1 = 0.15$, p = 1225 × 9.81^{-1} MPa, and c = −1.5. As for 12KhN3A steel [3], we assume k = 3, A = $4\tau_l$ and q = 0.75. The results of calculations are represented by the curves and the results of the experiment are represented by the points. To make comparison easier, the tension and compression diagrams are plotted in coordinates of the stress intensity σ_i against the strain intensity ε_i. The small circles represent uniaxial stretching of specimen No. 4−028 ($\sigma_z > 0$, $\sigma_\varphi = 0$), the dark circles are for stretching in a circumferential direction of specimen No. 4−118 ($\sigma_\varphi > 0, \sigma_z = 0$), and the right triangles are for equal biaxial stretching specimen No. 4−043 ($\sigma_z = \sigma_\varphi$, $\mu_\sigma = 1$). The diagrams of pure shear are plotted in coordinates of the maximum shear stress τ_m against the maximum shear γ_{max}($\gamma_{max} = \gamma_{max}^e + \Gamma_{max}$, γ_{max}^e is the elastic component of the shear strain, found using Hooke's law). The test made on specimen No. 4−115 correspond to this state with $\sigma_z = 2\sigma_\varphi$ (the stars) and specimen No. 4−041 for $\sigma_\varphi = -\sigma_z$ (the dark triangles). In addition, on the $\tau_m \sim \gamma_{max}$ diagram we show for comparison how the maximum shear develops in the case of uniaxial stretching (the light circles, specimen No. 4−028).

On the whole, the data on proportional loading confirms the fact that 40Kh steel in the test state is an initially isotropic material, having similar resistance to tension and compression and satisfying the yield criterion (3.3). The strengthening diagrams shown in Fig. 1 were taken as the nominal diagrams for this material for these forms of stressed state.

5. Figure 2 shows test data on loading along a two-section trajectory of specimen No. 4−078 (the points) which enable us to determine the parameter a_1 (Eq. (3.2), the curves).

The first part of the loading consisted of uniaxial stretching up to a stress of $\sigma_z = 42 \times 9.81^{-1}$ MPa. Over this section of proportional loading the reduction coefficient k_r [3] of the strengthening diagram of the material of this specimen to the nominal diagram was determined; it turned out that k_r equals 1.09 (the values of the stresses that are fixed during the test used to calculate the values of the plastic deformation components must be multiplied by this coefficient).

We then made a break in the loading trajectory after which, for a constant ratio of the increments of the stresses $\Delta\sigma_\varphi/\Delta\sigma_z = 2.5$, we have $\dot{\tau}_m > 0$, $\dot{\tau}_{12} < 0$, $\dot{\tau}_{23} > 0$. The experimental values of the stresses, the components of the strain (their plastic components), and also σ_i and τ_{ij} at several points are given in the table. Comparison of the values of Γ_z and Γ_φ shows that after the break in the trajectory the component of the strain $\Gamma_i^\varphi = \Gamma_z$ increases, while the component $\Gamma_2 = \Gamma_\varphi$ undergoes practically no increment up to the 15-th point of readout, beginning from which Γ_2 also increases. At this instant, as was shown above, condition (3.4) must be satisfied, which gives $a_1 = 0.15$ for $\tau_{23}^0 = 6.81 \times 9.81^{-1}$ MPa.

We will note one more feature of the behavior of a material outside the elastic limit, revealed in this experiment. After a break in the loading trajectory on a certain part of its second section, the stress intensity actually remains constant, but nevertheless an increment in the plastic deformation is recorded ($\dot{\Gamma}_1 = \dot{\Gamma}_z > 0$, see Table 1). This result agrees with the observations in [9] and elsewhere, which detected an increment in the plastic deformation for loadings when the value of the second invariant of the stress deviator remains unchanged, and only the form of the stressed state varies.

Experimental data also confirm that, beginning from the 15th readout point (see Table 1) of the measured quantities, there is a positive increment in the deformation component $\Gamma_2 = \Gamma_\varphi$. This indicates that slipping over the area T_{23} is occurring.

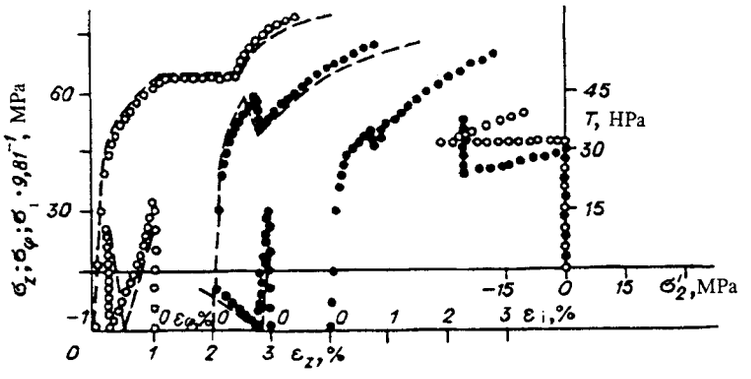

Fig. 5

According to (2.4), the increment in the shear $d\Gamma_2 > 0$, when there are no slippings over the areas T_{12} or they develop with lesser intensity than over the areas T_{23}, while the shear stresses τ_{12} and τ_{23} are related by the inequality $\tau_{23} > \tau_{12}$. However, the latter is only satisfied after the 19-th point. This raises doubts about the correctness of (2.2) between the increments of the deformation from the main and additional slippings in the place of complex loading. They can be refined as follows.

Using the assumption that, on each area of slipping T_{ij} the resistance to shear has the form (2.1), we can determine the apertures θ_{ij} of the fans of slippings on these areas at the current instant of time t. As follows from the above, at the instant t_* when the break in the loading trajectory occurs $\theta_{13} = \theta_{12} = \theta_* (\theta_{23} = 0)$. When $t > t_*$, it turns out that $\dot{\theta}_{12} = 0$ and the increment in the slipping intensity $\dot{r}_{12} = 0$ up to the 15-th point of readout, and then $\dot{r}_{12} > 0$, but the boundaries of the fan of slippings over the given area is less than at the instant t_*. This suggests the following conclusion: the contribution to deformation from these additional slippings is less when the fan of slippings is partially "frozen."

We will put

$$\tau_{12} - \psi(\tau_0, m) = R_{12}.$$

The instant when slippings over the area T_{12} are resumed is found from the condition

$$R_{12}/\Psi(\tau_0, m) = R_{12}^*/\Psi^*(\tau_0, m)$$

(the asterisks denote quantities at the instant t_*).

The fan of slippings at the current instant of time will encompass the whole fan at the preceding instants when the following equation is satisfied:

$$R_{12}|_{t>t_*} = R_{12}^*.$$

An analysis of these experiments enabled us to obtain an approximation of the relationship between the increments of the shears and the main and additional slippings

$$d\Gamma_1^d = k_{12}(\tau_{12}/\tau_m)^q d\Gamma_1^0, \quad d\Gamma_3^d = k_{23}(\tau_{23}/\tau_m)^q d\Gamma_3^0,$$

where

$$k_{12} = 1 - (R_{12}^* - R_{12})/R_{12} \text{ for } R_{12} \leq R_{12}^*, \; k_{12} = 1 \text{ for } R_{12} > R_{12}^*.$$

the coefficient k_{23} is found in the same way as the coefficient k_{12}.

Hence, a simple method has been developed for determining the parameters of the material used in the slipping model. Theoretical curves have been drawn for different complex loadings. Below we will present a very different testing program.

6. In Fig. 3 the loading trajectory is shown in $T-\sigma_2'$ coordinates ($\sigma_2' = T_{23} - T_{12} = T\mu_\sigma$). Here the light circles represent the complex loading of specimen No. 4−017 ($k_l = 1.09$), and the dark circles represent proportional loading of specimen No. 4−069 ($k_l = 1.09$). The final values of the stresses in both cases were the same and, as can be seen from the experimental diagrams, the final values of the deformation components were also the same. Consequently, the influence of the

break in the loading trajectory in this case attenuates rapidly. This always occurs when all three principal shear stresses increase during loading and give a monotonic increase in the slipping fans.

The monotonic development of slippings over the area T ($\theta > 0$) imposes a limitation on the increments of the principal stresses

$$\frac{d\sigma_1}{d\sigma_2} > \frac{2(2\sigma_2 - \sigma_1)(\tau_m + 4\tau_l)}{[9m\tau_0 - 2(2\sigma_1 - \sigma_2)]\tau_m - [3(5 + 3m_1)\tau_0 + 8(2\sigma_1 - \sigma_2)]\tau_l}.$$

We similarly also checked the condition for the increase in the slipping fans to be monotonic over the other areas (T_{12} and T_{23}).

As we know, small sign-varying deviations (with respect to the parameter μ_σ) from proportional loading for any form of stress state lead to small deviations in the deformation corresponding to the given μ_σ. This was confirmed from tests on specimen No. 4−070 (the light circles in Fig. 4, $k_l = 1.09$). For comparison Fig. 4 also shows a diagram of $\varepsilon_z = \varepsilon_z(\sigma_z)$ for pure shear (the continuous curve, specimen No. 4−115).

The only difference in this experiment is that on changing from a state of uniaxial tension to a state of pure shear, the loading history was found to have a considerable influence (Fig. 4, the dark circles − specimen No. 4−108, $k_l = 1.05$). According to the above model, after the break in the loading trajectory in this case, slippings over the area T_{23} occur when the local yield point τ_{23}^0 satisfying condition (3.4) is reached. In this case $\tau_{23}^0 \approx 3.5 \times 9.81^{-1}$ MPa. This "lag" in the slipping over the area T_{23} behind the development of slippings over the other areas (T and T_{12}) leads to a constant increase (in modulus) of the deformation $\Gamma_2 = \Gamma_\varphi$, although less intense for uniaxial tension, but is maintained until a state of pure shear is achieved.

A somewhat different pattern occurs in the change in deformations when the opposite transition is made, namely, from pure shear to uniaxial stretching (Fig. 4, specimen No. 4−100 − the triangles, $k_l = 1.02$). The difference between the deformation components in a small neighborhood of the yield point when $\mu_\sigma = -1$ and $\mu_\sigma = 0$ is small. It is practically erased as the level of stresses increases for the loading trajectory indicated for specimen No. 4−100 as $\mu_\sigma \to -1$. This occurs by virtue of the predominance of slippings over the areas T and T_{12}.

The loading trajectory of specimen No. 4−100 contains a third section: after reaching a state of uniaxial stretching the reverse transition occurred from $\mu_\sigma = -1$ to $\mu_\sigma = 0$ (however the state $\mu_\sigma = 0$ was not reached: due to the presence of a fairly large overall deformation of the specimen the experiment was discontinued). A characteristic feature is that at the beginning of the third stage of deformation the hardening of the material increases sharply, approaching the elastic deformation (see Fig. 4), and the hardening diagram $\sigma_z = \sigma_z(\varepsilon_z)$ then becomes similar to the diagram for pure shear (when $\sigma_z = 2\sigma_\varphi$). This can be explained by the fact that when the stress state changes the value of the invariant m decreases, the function $\psi(\tau_0, m)$ on a certain part of the third section of the loading trajectory remains constant, while the function $\psi(\tau_0, m)$ decreases much less than in the preceding stages. As a result, the slipping intensity over this part increases only slightly. Its increment begins to increase when the function $\psi(\tau_0, m)$ once again decreases as the stress level increases.

A change in the deformations and the nature of the hardening, similar to that described for specimen No. 4−100, was also observed in the case of a transition from pure shear to uniaxial tension for constant maximum shear stress (Fig. 5, specimen No. 4−13, (the light circles, $k_l = 1.05$). These experimental results reinforced the conclusion that the function $\psi(\tau_0, m)$ plays a considerable role in the resistance to shear of the form (2.1).

An increment in the plastic deformation in the case of a transition from $\mu_\sigma = 0$ to $\mu_\sigma = -1$ also occurs when there is some reduction in the maximum shear stress due to a reduction in the intensity of the stresses σ_i − the "dividing duck" on the $\sigma_i = \sigma_i(\varepsilon_i)$ diagram. This was observed in tests on specimen No. 4−133 (Fig. 5, the dark circles, $k_1 = 1.05$). An analysis of the experimental data showed that in this case the unloading on the areas T_{12}, for which, at the end of the second loading section, $\Delta\Gamma_z \approx 0.1\%$ and $\Delta\Gamma_\varphi \approx -0.1\%$, i.e. $\Delta\Gamma_1 = -\Delta\Gamma_2$ and, consequently, $\Delta\Gamma_3 = 0$. In other words, for loading along the second section of the trajectory, plastic deformation is due solely to slippings over the area T_{12} when they are not present ("frozen") over the other two areas. This also follows from the model representations and was used in the calculation.

Hence, the model of a material based on representations of the principal slipping areas is completely justified. The variety of complex-loading effects considered reveal quite clearly the "switching in" and "switching out" of these areas for different changes in the stress states. The resistance to shear (slipping), taken as the main strength characteristic of the material for plastic deformation, enables one to determine the deformation anisotropy that occurs quite reliably.

REFERENCES

1. A. A. Vakulenko, "The connection between the micro- and macroproperties in elastoplastic media," in: Results of Science and Technology, Vol. 22, Ser. MDTT, VINITI, Moscow (1991).
2. R. A. Vasin, "The governing relations in the theory of plasticity," in: Results of Science and Technology, Vol. 21, Ser. MDTT, VINITI, Moscow (1990).
3. V. M. Zhigalkin, B. A. Rychkov, and O. M. Usova, "The characteristics of the plastic deformation of steel on loading and partial unloading," Preprint Inst. Avtomatiki, Akad. Nauk KirgSSR, Frunze (1991).
4. M. Ya. Leonov, E. B. Nisnevich, and B. A. Rychkov, "A plane theory of plasticity based on the synthesis of slippings," Izv. Akad. Nauk SSSR. MTT, No. 6 (1979).
5. E. I. Shemyakin, "Anisotropy of the plastic state," in: Numerical Methods of the Mechanics of a Continuous Medium [in Russian], Vol. 4, No. 4, VTs SO Akad. Nauk SSSR, Novosibirsk (1973).
6. S. A. Khristianovich, "Deformation of a hardened plastic material," Izv. Akad. Nauk SSSR, MTT, No. 2 (1974).
7. B. Pohl, "Macroscopic criteria of plastic flow and brittle fracture," in Fracture. Mathematical Principles of Fracture, Vol. 2, Chapter 4 [in Russian], IL, Moscow (1975).
8. V. M. Zhigalkin, "The nature of the hardening of a plastic material. Communications 1 and 2," Problemy Prochnosti, No. 2 (1980).
9. G. A. Doshchinskii and A. M. Koreneva, "Plastic flow under constant stress intensity," Izv. Akad. Nauk SSSR, MTT, No. 5 (1970).